

# Study of Scintillator Strip with Wavelength Shifting Fiber and Silicon Photomultiplier.

V.Balagura <sup>a</sup> M.Danilov <sup>a</sup> B.Dolgoshein <sup>b</sup> S.Klemin <sup>b</sup>  
 R.Mizuk <sup>a</sup> P.Pakhlov <sup>a</sup> E.Popova <sup>b</sup> V.Rusinov <sup>a</sup>  
 E.Tarkovsky <sup>a</sup> I.Tikhomirov <sup>a</sup>

<sup>a</sup>*Institute for Theoretical and Experimental Physics, B.Cheremushkinskaya 25,  
 Moscow, 117259, Russia*

<sup>b</sup>*Moscow Engineering and Physics Institute, Kashirskoe sh. 31, Moscow, 115409,  
 Russia*

---

## Abstract

The performance of the  $200 \times 2.5 \times 1$  cm<sup>3</sup> plastic scintillator strip with wavelength shifting fiber read-out by two novel photodetectors called Silicon PhotoMultipliers (SiPMs) is discussed. The advantages of SiPM relative to the traditional multichannel photomultiplier are shown. Light yield and light attenuation measurements are presented. This technique can be used in muon or calorimeter systems in which tracking information is also required.

*Key words:* Scintillation detectors, wavelength shifting fibers, silicon photomultiplier

*PACS:* 29.40Mc, 29.40Vj

---

The detection of charged particles with plastic scintillators, wavelength shifting (WLS) fibers and multichannel photomultipliers is a well known, efficient and robust technique (see, e.g. [1]). However it has severe limitations. First, photomultipliers can not work in the magnetic field. For scintillator counters inside a magnet one should bring the light out of it by clear fibers. This complexifies the detector and leads to some light losses. Second, fibers from different scintillator counters should be assembled together in a bundle attached to the multichannel photomultiplier. This is not always easy to arrange. Finally, calibration and monitoring of a multichannel photomultiplier is not a simple task.

In this work performed at ITEP (Moscow) we use the novel photodetector called Silicon Photomultiplier (SiPM) [2] instead of the traditional photomultiplier. It is the matrix of  $1024 = 32 \times 32$  tiny independent silicon photodiode

pixels placed in the area of  $1 \times 1 \text{ mm}^2$  and working in a Geiger mode. Each diode has its own quenching resistor of the order of a few hundred  $\text{k}\Omega$ . The characteristics of individual pixels and their discharge signals are almost the same. A typical amplification which depends on the applied voltage is of the order of  $10^6$ . The signals from all pixels are intrinsically summed up. The total SiPM response is thus proportional to the number of incident photons as long as there is no saturation, i.e. the number of fired pixels is small in comparison with the total number of pixels in the SiPM (1024 in our case <sup>1</sup>). The photodetection efficiency depends on the light wave length and the applied voltage. Typical values are around  $\approx 10\text{--}15\%$ . Thus SiPM and traditional photomultipliers have similar gain and efficiency. However, SiPM is approximately twice cheaper than one channel in the multichannel photomultiplier. In addition it can work in the magnetic field, so there is no need in the clear fibers. SiPM is so tiny that can be mounted directly on the detector without efficiency loss. We install two SiPMs at the scintillator strip ends (see Fig. 1).

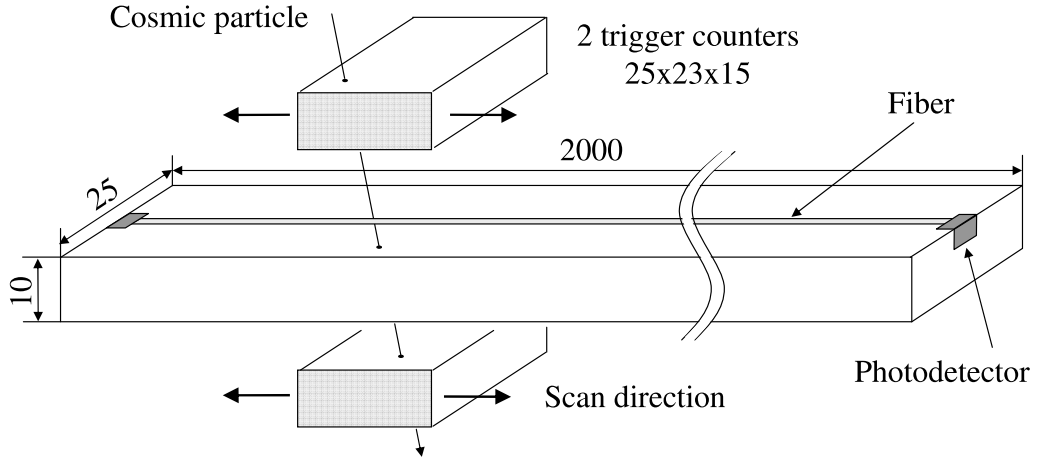


Fig. 1. The layout of the test bench (not in scale). The sizes are in mm.

The scintillator strip is produced in Vladimir (Russia) by the extrusion technique from the granulated polystyrene with two dyes (1.5% of PTP and 0.01% POPOP). Its sizes are  $200 \times 2.5 \times 1 \text{ cm}^3$ . The Kuraray multiclading WLS fiber Y11 (200) with 1 mm diameter is put in the 2.5 mm deep groove. To enlarge the light output, the strip is wrapped in the Superradiant VN2000 foil produced by the 3M company. No gluing is used to attach the WLS fiber to the SiPM or to the strip. There is about  $200 \mu\text{m}$  air gap between the fiber end and the SiPM to ensure that the fiber can not scratch the SiPM surface.

We use the cosmic particle trigger consisted of a pair of  $2.3 \times 2.5 \text{ cm}^2$  scintillator counters placed above and below the strip (see Fig. 1). The SiPM spectra like the one shown in Fig. 2a, are obtained for different positions of the trigger counters along the strip.

<sup>1</sup> SiPMs can be produced with different number of pixels in the range 500–3000.

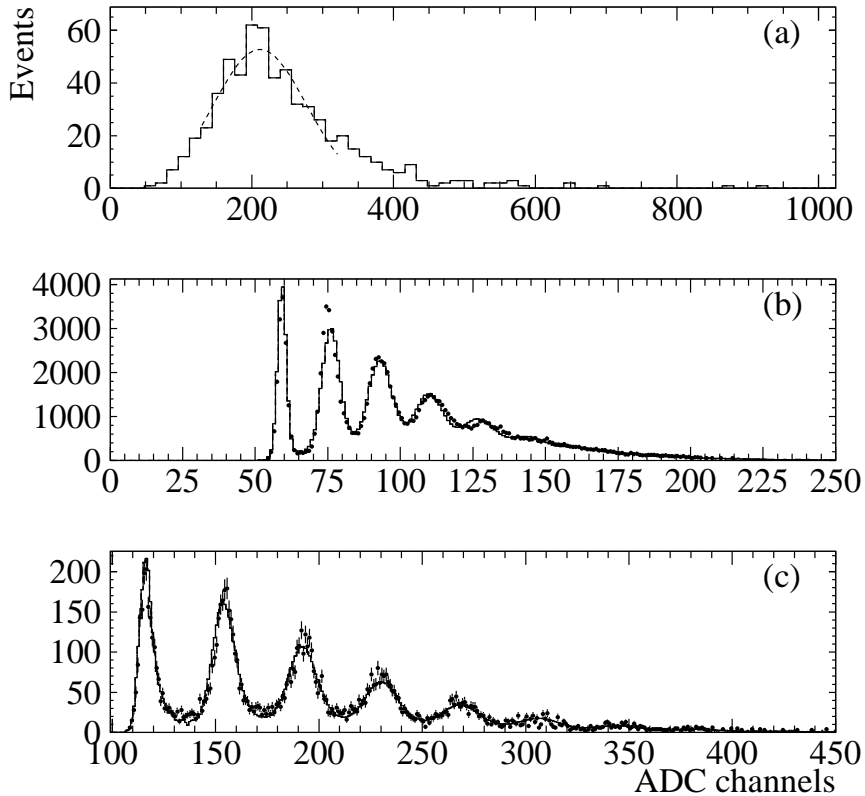


Fig. 2. SiPM ADC spectra. (a): Typical SiPM response to cosmic particles. The dashed line shows the fit of the peak central region to the Gaussian distribution. (b): The same SiPM is illuminated by the LED light, (c): the same as (b) but for another SiPM produced recently with improved technology. The fit curve is described in detail in Appendix A.

In each case the region around the peak is fit to the Gaussian distribution as shown in Fig. 2a. The central value of the Gaussian is transformed into the average number of fired SiPM pixels using the SiPM gain determined in the following way. The strip is illuminated periodically by the short flashes of the Light Emitting Diode (LED). The corresponding SiPM response spectrum shown in Fig. 2b is collected in parallel to the cosmic ray data. The LED flash is chosen in such a way that each time only a few SiPM pixels are fired. Since the signals from different pixels are very similar, one can see clear peaks corresponding to different number of fired pixels. The distance between the peaks thus measures the SiPM gain. For larger number of incident photons like in Fig. 2a the individual peaks become smeared.

The cosmic particles selected by the two trigger counters are not strictly vertical. Thus they produce slightly more scintillation light than the minimum ionizing particle at normal incidence to the strip. To correct for this effect,

we made a simple simulation assuming that the angular distribution of all cosmic particles coincided with the one of cosmic muons and had the form  $\cos^2 \theta$  where  $\theta$  was the angle with respect to the vertical direction [3]. In this way it was found that in average the path length of triggered particles inside the scintillator was  $1.1 \times 1$  cm, i.e. 1.1 times larger than the strip thickness. Assuming that the light yield was also 10% larger, all experimental numbers were divided by 1.1.

There is another effect which should be taken into account in determining the light yield. The procedure described above allows to measure the average number of fired SiPM pixels. It is not equal to the number of detected photons. One photon can fire more than one pixel due to the SiPM interpixel “cross talk”. This effect increases with the applied voltage. In our case the average number of pixels fired by one initial photoelectron is about 1.43 for the left SiPM and 1.28 for the right one. It is determined from the fit of the spectrum in Fig. 2b described in detail in Appendix A. The “cross talk” is found from the deviation of the distribution of the number of fired pixels from the Poisson law. After correction for the “cross talk” effect, the resulting average number of detected photons measured from each strip end is shown in Fig. 3 by filled triangles and open squares for different positions of the trigger counters. One can see that for the 2 m strip the attenuation at the far end is about 50%. The upper points in Fig. 3 show the sum of two SiPM signals. It is uniform within  $\pm 13\%$ . In the worst case when the particle passes through the strip center there are more than 13 detected photons. In case of Poisson statistics this corresponds to 98% efficiency at the threshold  $\geq 7$  photons or  $\geq 8$  fired pixels. With this requirement the efficiency averaged over the strip exceeds 99%.

These efficiency estimations can be also checked with the data. The distribution of the number of pixels fired in two SiPMs by a cosmic particle is shown in Fig. 4. Top and bottom spectra correspond to two extreme cases when the particle passes through the end or the center of the strip. A few events around zero belong to the pedestal which appears here due to imperfection of the trigger. The plots are not corrected for the factor 1.1 which was introduced above to take into account not normal incidence of cosmic particles. Therefore to estimate the inefficiency of the requirement to have  $\geq 8$  fired pixels for normal incidence one should count the entries between the pedestal and the value  $8 \cdot 1.1 \approx 9$ . This part of the spectrum is hatched. There are 11 such events on the top plot. They correspond to 1.7% of inefficiency which agrees with the calculations above. The inefficiency averaged over all other positions of trigger counters along the strip is found to be 0.7%. Note that in determining the light yield in Fig. 3 the position of the peak center in the signal amplitude spectrum is used. It is lower than the mean value of the histogram. E.g. for the strip center the mean value of the top spectrum in Fig. 4 is equal to 24.5 while the peak center is at 20.7 fired pixels.

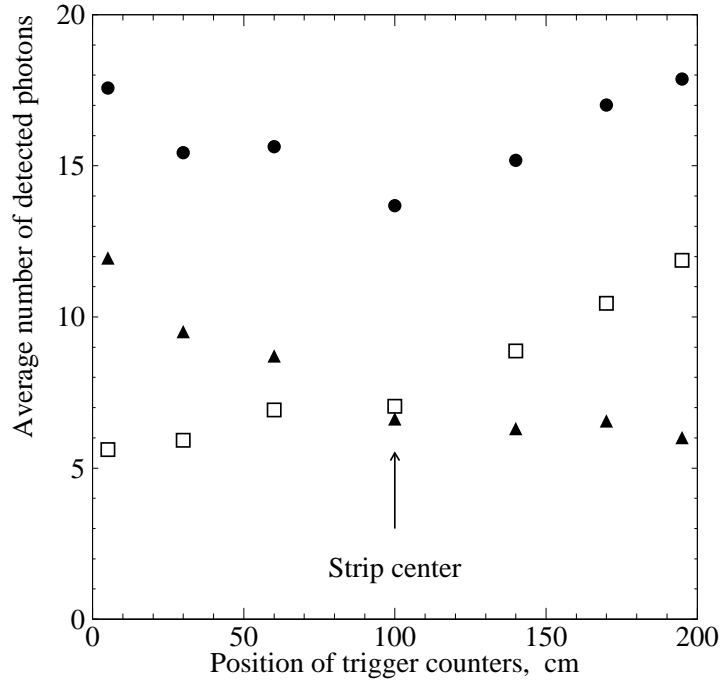


Fig. 3. *Average number of photons detected by SiPM for normally incident cosmic ray particle versus the position of the trigger counters along the strip. The upper curve (filled circles) is the sum of the two lower curves which correspond to the left (filled triangles) and right (open squares) SiPMs.*

The typical SiPM noise rate recorded without any trigger exponentially depends on the threshold (see Fig. 5). With the lowest threshold corresponding to one half of the SiPM pixel signal it is about 2 MHz at room temperature. The rate of two SiPMs put in the coincidence depends on the type of the electronics. For example one can simply set the threshold for the sum of two SiPM signals integrated during the same 120 nsec time interval which is used in obtaining the amplitude spectra in Fig. 4. The probability to get in this way  $\geq 8$  fired pixels due to noise is measured to be  $7 \cdot 10^{-4}$ . Clearly it can be suppressed even further if the electronics utilizes the fact that two SiPM signals caused by real particles are closer in time than 120 nsec. To estimate the noise rate dependence on the time window we made a simple simulation. The distribution in Fig. 5 was differentiated to get the amplitude spectrum of one SiPM noise signal. The number of signals within the given time window was allowed to fluctuate according to the Poisson statistics. In this way for 120 nsec window the probability to get  $\geq 8$  fired pixels was found to be  $1 \cdot 10^{-4}$  instead of  $7 \cdot 10^{-4}$  in data. The discrepancy may indicate the presence of the unknown extra source of background in our cosmic ray setup. For 50 nsec time window the probability in the simulation was found to be  $1.1 \cdot 10^{-5}$ , i.e. about an order of magnitude lower than that for 120 nsec. Thus it is possible to reduce drastically the noise rate by using shorter gate.

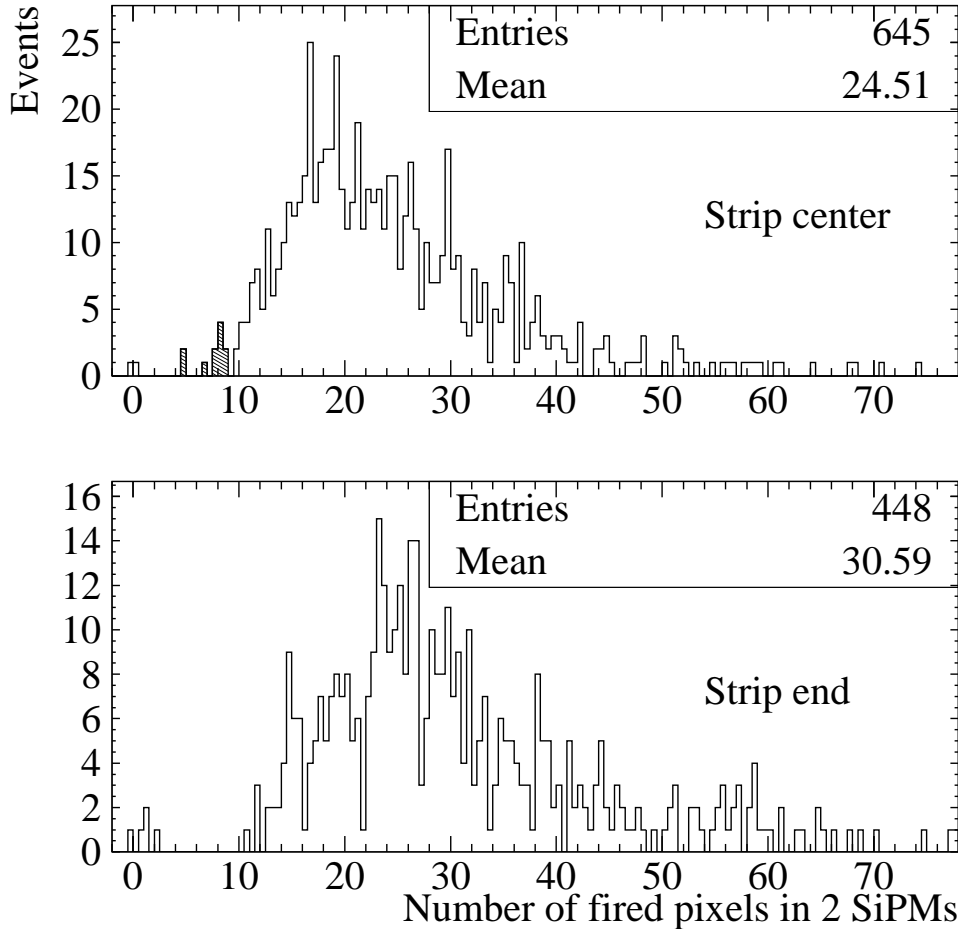


Fig. 4. Number of fired pixels in two SiPMs when trigger counters are located at the strip center and at the ends.

In conclusion, the detector consisting of the  $200 \times 2.5 \times 1$  cm<sup>3</sup> plastic scintillator strip, the wavelength shifting fiber and two novel photodetectors called Silicon PhotoMultipliers has been constructed and tested. A possibility to use such a new technique in the muon systems or calorimeters with tracking information has been demonstrated. For example it can be used in the muon system of the future International Linear Collider detector. SiPM has similar gain and efficiency as the traditional multichannel photomultiplier. It also has several advantages. There is no need to use clear fibers to bring the light out of the magnetic field or to arrange many fibers in one bundle attached to the multichannel photomultiplier. SiPM can be mounted directly on the strip end. Its gain can be determined easily by observing the peaks corresponding to different number of fired SiPM pixels (see Fig. 2b,c). Finally it is approximately twice cheaper than one channel in multichannel photomultiplier. Light yield and light attenuation measurements are shown in Fig. 3. The light yield of

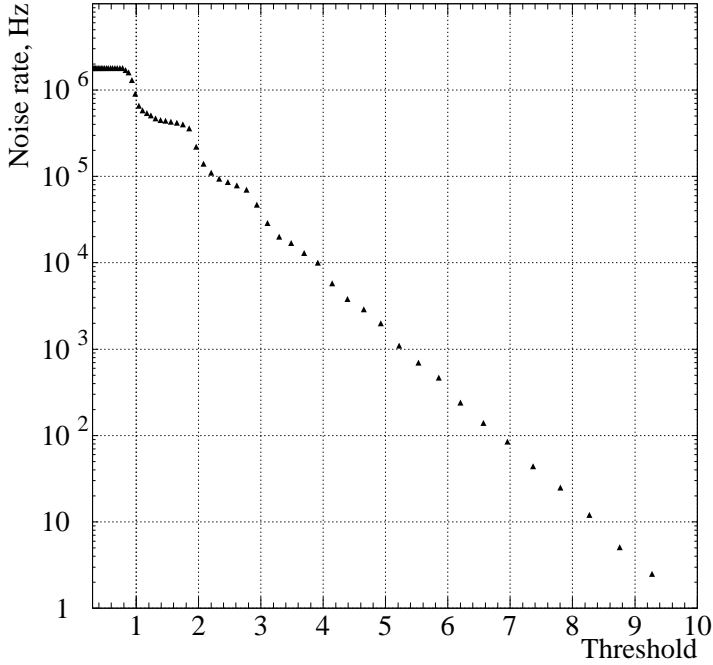


Fig. 5. *Typical SiPM noise rate versus the threshold expressed in the units corresponding to one pixel signals.*

more than 13 detected photons per cosmic ray particle at normal incidence is obtained. The light collection efficiency can be further increased by gluing the WLS fiber to the strip. We plan to study this possibility systematically in the future.

## A The fit procedure of the SiPM calibration spectrum

To calibrate the SiPM, it is illuminated by the LED flashes. The corresponding ADC spectrum of one of the SiPMs is shown in Fig. 2b. This histogram is fit to the convolution of the pedestal spectrum ( $B$ ) obtained when the LED is off and the SiPM response function ( $L$ ) to the photons from LED which will be described later. Thus its Fourier transform which will be denoted in the following by  ${}^F$  superscript can be written as  $B^F L^F$ . Assuming the stability of LED and the pure Poisson distribution of photons detected by SiPM,  $L^F$  can be written as

$$L^F = \sum_{n=0}^{+\infty} \frac{e^{-\mu} \mu^n}{n!} (P^F)^n = \exp\{\mu(P^F - 1)\},$$

where  $P^F$  is the Fourier transform of the response to exactly *one* photon,  $\mu$  is the average number of photons detected by the SiPM. We use the fact that the response to  $n$  photons is  $n$  convolutions of  $P$  and thus has a Fourier transform  $(P^F)^n$ . Due to the interpixel cross-talk one photon can fire more than one pixel. To describe this effect we approximate  $P^F$  by

$$P^F = \frac{G^F + \epsilon(G^F)^2 + \epsilon^2(G^F)^3 + \dots + \epsilon^{k-1}(G^F)^k + \dots}{1 + \epsilon + \epsilon^2 + \dots + \epsilon^{k-1} + \dots} = G^F \frac{1 - \epsilon}{1 - \epsilon G^F},$$

where  $\epsilon$  describes the amount of cross-talk,  $G^F$  is the Fourier transform of the SiPM signal distribution when exactly one random pixel in it is fired. The average number of pixels fired by one photon is  $1/(1-\epsilon)$ . As an approximation of  $G$  the Gaussian distribution is taken. Its sigma ( $\sigma$ ), mean ( $\Delta$ ) and also the cross-talk ( $\epsilon$ ) are the only fit parameters.  $\Delta$  is equal to the distance between adjacent peaks in Fig. 2a. The number of photons  $\mu$  is constrained in the fit by the condition that the average of the histogram in Fig. 2a should be equal to the average of the background histogram  $B$  plus the average of  $L$  which is  $\Delta\mu/(1-\epsilon)$ . Here we assume that the averages of experimental histograms when LED is on and off are known accurately and do not fluctuate.

If  $G$  and  $B$  functions are normalized so that they have unit integrals, the resulting formula for the Fourier transform of the fit function is

$$N \cdot B^F \exp\left\{\mu \frac{G^F - 1}{1 - \epsilon G^F}\right\},$$

where  $N$  is the total number of entries in the histogram. It is found that such a fit with 3 parameters can describe large variety of LED spectra for different SiPMs, bias voltages and LED intensities.

Due to improvements in production, the differences between individual pixel signals inside the SiPMs produced recently became smaller. Fig. 2c shows one typical example. The separation between the peaks is much clearer.

## References

- [1] P. Adamson *et.al.*, The MINOS scintillator calorimeter system, *IEEE Trans. Nucl. Sci.* **49** (2002) 861–863.
- A.Pla-Dalmau, Extruded plastic scintillator for the MINOS calorimeters, in: “Annecy 2000, Calorimetry in high energy physics”, proceedings of 9th Conference on Calorimetry in High Energy Physics (CALOR 2000, Annecy, France), 513–522, *preprint* FERMILAB-CONF-00-343, (2001) 1–11.

D.F.Anderson *et.al.*, Development of a low-cost extruded scintillator with co-extruded reflector for the MINOS experiment, *preprint* FERMILAB-CONF-00-261-E, (2000) 1–5.

[2] G.Bondarenko *et.al.*, Limited Geiger-mode silicon photomultiplier with very high gain, *Nucl. Phys. Proc. Suppl.* **61B** (1998) 347–352.  
G.Bondarenko *et.al.*, Limited Geiger-mode microcell silicon photodiode: new results, *Nucl. Instr. Meth.* **A442** (2000) 187–192.  
P.Buzhan *et.al.*, An advanced study of silicon photomultiplier, *ICFA Intstr.Bull.* **23** (2001) 28–41.  
P.Buzhan *et.al.*, Silicon photomultiplier and its possible applications, *Nucl. Instr. Meth.* **A504** (2003) 48–52.  
V. Andreev *et.al.*, A high granularity scintillator hadronic-calorimeter with SiPM readout for a Linear Collider detector, *preprint* DESY-04-143, LC-DET-2004-027 (2004) 1–17.

[3] S. Eidelman *et.al.*, Particle Data Group, *Phys. Lett.* **B592** (2004) 1.